Electronic Supplementary Information

Exploring new hydrated delta type vanadium oxides for lithium intercalation

Joseba Orive,[a,b] Roberto Fernández de Luis,[c] Edurne S. Larrea,[d] Ana Martínez-Amesti,[e] Angela Altomare,[f] Rosanna Rizzi,[f] Luis Lezama,[d] María I. Arriortua,[c,d] Juan Luis Gómez-Cámer,[g,h] María Jauregui,[h] Montse Casas-Cabanas,[h] Judit Lisoni[b,i]*

[a] Dpto. de Ingeniería Química, Biotecnología y Materiales, FCFM, Universidad de Chile, Av. Beauchef 851, Santiago 8370448, Chile.

[b] NM MultiMat, Chilean Ministry of Economy, Development and Tourism.

[c] BCMaterials (Basque Centre for Materials, Applications & Nanostructures), Bld. Martina Casiano, 3rd. Floor UPV/EHU Science Park, Barrio Sarriena s/n, 48940 Leioa, Spain.

[d] Dpto. de Mineralogía y Petrología and Dpto. de Química Inorgánica, Facultad de Ciencia y Tecnología, Universidad del País Vasco UPV/EHU, Sarriena s/n 48940 Leioa, Spain.

[e] SGIker, Servicios Generales de Investigación UPV/EHU, Avda. Tolosa 72, 20018 Donostia-San Sebastian, Spain.

[f] Institute of Crystallography-CNR, via Amendola 122/o, Bari, Italy.

[g] Dpto. de Química Inorgánica e Ingeniería Química, Universidad de Córdoba, 14071 Córdoba, Spain.

[h] CIC Energigune, Parque Tecnológico de Álava, Albert Einstein 48, 01510 Miñano, Spain.

[i] Instituto de Ciencias Físicas y Matemáticas, Facultad de Ciencias, Universidad Austral de Chile, Valdivia, Chile.

* Corresponding author: joseba.orive@ing.uchile.cl
Phone: +56 229771076.

Table S1. ICP-Q-MS and elemental analyses (%) of **NaVOx**, **KVOx** and **NHVOx**.

Sample	V exp	V calc	Na exp	Na calc	K exp	K calc	N exp	N calc
$Na_{0.35}V_2O_5{\cdot}0.8(H_2O)$ (**NaVOx**)	49.2(5)	49.86	3.95(4)	3.94	-------	-------	-------	-------
$K_{0.36}(H_3O)_{0.15}V_2O_5$ (**KVOx**)	51.1(4)	51.25	-------	-------	7.05(5)	7.08	-------	-------
$(NH_4)_{0.37}V_2O_5{\cdot}0.15(H_2O)$ (**NHVOx**)	53.6(4)	53.27	-------	-------	-------	-------	2.73(5)	2.71

Table S2. Pattern Matching and Rietveld refinement parameters for **NaVOx**, **NaVOx_HT**, **KVOx** and **NHVOx**.

Sample	**NaVOx**		**NaVOx_HT (110ºC)**		**KVOx**		**NHVOx**	
Formula	$Na_{0.35}V_2O_5{\cdot}0.8(H_2O)$		$Na_{0.35}V_2O_5{\cdot}0.23(H_2O)$		$K_{0.36}(H_3O)_{0.15}V_2O_5$		$(NH_4)_{0.37}V_2O_5{\cdot}0.15(H_2O)$	
M. Weight (g/mol)	204.34		194.07		198.81		191.26	
Z	2		2		2		2	
Analysis Method	*Pattern Matching*	*Rietveld Analysis*	*Pattern Matching*	*Rietveld Analysis*	*Pattern Matching*	*Rietveld Analysis*	*Pattern Matching*	*Rietveld Analysis*
a, Å	11.9157(2)	11.925(1)	11.6862(4)	11.863(3)	11.9055(2)	11.9057(5)	11.8798(2)	11.8807(3)
b, Å	3.74152(5)	3.7415(1)	3.7272(1)	3.7160(5)	3.77266(6)	3.7716(2)	3.76855(4)	3.76875(7)
c, Å	14.2111(4)	14.239(1)	12.3832(3	12.543(2)	13.1062(3)	13.092(1)	12.6074(2)	12.6044(4)
β, º	114.053(3)	114.296(8)	115.844(2)	117.32(2)	117.331(1)	117.354(4)	110.207(2)	110.160(3)
V, Å^3	578.56(2)	579.06(7)	485.42(3)	491.3(2)	522.96(2)	522.15(5)	529.69(1)	529.79(3)
Reflections	739	741	625	628	670	670	678	679
R_{Bragg}	0.11	13.4	0.05	25.2	0.19	17.1	0.04	16.4
R_f	0.504	10.2	0.580	23.0	0.275	14.6	0.197	14.6
R_p	14.5	28.0	19.8	38.1	17.1	30.2	17.0	28.7
R_{wp}	15.0	30.5	19.1	40.1	18.1	32.0	19.0	29.4
R_{exp}	3.70	3.73	4.58	4.58	3.73	3.79	3.46	3.57
χ^2	16.44	66.90	17.38	76.61	23.59	71.21	30.03	67.90

Table S3. Rietveld refined atomic coordinates and equivalent isotropic displacement parameters, B_{iso} (Å^2) of **NaVOx**, **NaVOx_HT**, **KVOx** and **NHVOx**.

NaVOx

Atom	**x**	**y**	**z**	**B_{iso} (Å^2)**	**Occ. F.**
V1	0.1249(9)	0.0	0.0992(6)	0.51(6)	0.5
V2	-0.1839(9)	0.0	0.1004(8)	0.51(6)	0.5
O1	0.183(4)	0.0	0.239(3)	0.5(2)	0.5
O2	-0.033(4)	0.0	0.0835(13)	0.5(2)	0.5
O3	0.3163(16)	0.0	0.0855(14)	0.5(2)	0.5
O4	0.1249(18)	0.0	0.1230(20)	0.5(2)	0.5
O5	-0.107(3)	0.0	0.252(3)	0.5(2)	0.5
O6W	0.290(3)	0.0	0.389(2)	2.224(3)	0.5
O7W	0.582(10)	0.0	0.674(4)	2.224(3)	0.17(2)
Na1	0.5	0.0	0.5	2.224(3)	0.235(9)

Table S3. Continuation.

NaVOx_HT (110ºC)

Atom	x	y	z	B_{iso} (Å^2)	Occ. F.
V1	0.1294(7)	0.0	0.1247(6)	0.5	0.5
V2	-0.1782(7)	0.0	0.1039(6)	0.5	0.5
O1	0.209(7)	0.0	0.2868(9)	0.5	0.5
O2	-0.0545(7)	0.0	0.0581(8)	0.5	0.5
O3	0.2609(11)	0.0	0.0539(8)	0.5	0.5
O4	0.153(3)	0.5	0.147(4)	0.5	0.5
O5	-0.087(7)	0.0	0.2664(11)	0.5	0.5
O6W	0.33160	0.5	0.43000	0.5	0.5
Na1	0.08760	-0.8970	0.41440	0.5	0.69(1)

KVOx

Atom	x	y	z	B_{iso} (Å^2)	Occ. F.
V3	0.4745(9)	0.0	0.1018(7)	0.51	0.5
V4	0.7978(8)	0.0	0.1120(6)	0.51	0.5
O8	0.596(3)	0.0	0.061(2)	0.51	0.5
O9	0.878(3)	0.0	0.2545(14)	0.51	0.5
O10	0.567(3)	0.0	0.304(2)	0.51	0.5
O11	0.317(3)	0.0	0.1027(15)	0.51	0.5
O12	0.460(3)	0.5	0.124(2)	0.51	0.5
O13W	0.305(3)	0.0	0.371(2)	0.51	0.5
K1	0.2964(15)	-0.396(3)	0.4058(11)	0.51	0.45(1)

NHVOx

Atom	x	y	z	B_{iso} (Å^2)	Occ. F.
V1	0.1144(7)	0.5	0.1177(6)	0.49	0.5
V2	-0.1907(6)	0.5	0.1170(5)	0.49	0.5
O1	0.1698(19)	0.5	0.2701(16)	0.49	0.5
O2	-0.0650(14)	0.5	0.0899(13)	0.49	0.5
O3	0.2719(20)	0.5	0.0886(15)	0.49	0.5
O4	0.1394(19)	1.0	0.1561(16)	0.49	0.5
O5	-0.1328(19)	0.5	0.2904(17)	0.49	0.5
O8W	0.027(2)	0.5	0.3297(17)	0.49	0.5
N1	0.197(2)	1.0	0.314(2)	0.49	0.5

Table S4. Coordination environment bond distances (Å) for **NaVOx**, **NaVOx_HT**, **KVOx** and **NHVOx** from the Rietveld analysis.

NaVOx

(V1)-(O1)^{i}	1.82(4)	(V2)-(O2)^{i}	1.91(5)	(O6W)-(O1)^{i}	2.73(3)	(O7W)-(O1)^{ii}	2.56(12)
(V1)-(O2)^{i}	1.80(5)	(V2)-(O3)^{ii}	2.462(19)	(O6W)-(O1)^{i}	2.73(3)	(O7W)-(O5)^{vi}	2.11(3)
(V1)-(O2)^{ii}	2.371(18)	(V2)-(O3)^{v}	1.883(3)	(O6W)-(O5)^{v}	2.70(6)	(O7W)-(O5)^{vi}	2.11(3)
(V1)-(O3)^{i}	2.37(2)	(V2)-(O3)^{v}	1.883(3)	(O6W)-(O7W)^{ii}	2.79(9)	(O7W)-(Na1)^{i}	2.93(4)
(V1)-(O4)^{i}	1.901(6)	(V2)-(O4)^{v}	2.43(3)	(O6W)-(Na1)^{i}	2.35(3)		
(V1)-(O4)^{i}	1.901(6)	(V2)-(O5)^{i}	1.97(4)				

NaVOx_HT (110ºC)

(V1)-(O1)^{i}	1.807(12)	(V2)-(O2)^{i}	1.805(14)	(O6W)-(O1)^{i}	2.53	(Na1)-(O1)^{i}	2.63
(V1)-(O2)^{i}	1.945(11)	(V2)-(O3)^{ii}	1.760(11)	(O6W)-(O1)^{i}	2.53	(Na1)-(O5)^{i}	2.09
(V1)-(O2)^{ii}	2.044(12)	(V2)-(O3)^{v}	1.988(4)	(O6W)-(O5)^{v}	2.64		
(V1)-(O3)^{i}	2.120(17)	(V2)-(O3)^{v}	1.988(4)	(O6W)-(Na1)^{vi}	1.78		
(V1)-(O4)^{i}	1.881(5)	(V2)-(O4)^{v}	2.30(5)	(O6W)-(Na1)^{vii}	1.78		
(V1)-(O4)^{i}	1.881(5)	(V2)-(O5)^{i}	1.817(15)				

KVOx

(V3)-(O8)^{i}	1.76(4)	(V4)-(O8)^{i}	2.18(4)	(O13W)-(O9)^{v}	2.80(4)	(K1)-(O9)^{v}	2.61(4)
(V3)-(O8)^{ii}	1.90(3)	(V4)-(O9)^{i}	1.660(17)	(O13W)-(O9)^{v}	2.80(4)	(K1)-(O10)^{v}	2.46(3)
(V3)-(O10)^{i}	2.35(3)	(V4)-(O11)^{ii}	2.498(19)	(O13W)-(K1)^{i}	1.578(16)	(K1)-(O13W)^{i}	2.335(14)
(V3)-(O11)^{i}	1.88(4)	(V4)-(O11)^{v}	1.910(6)	(O13W)-(K1)^{i}	2.335(14)	(K1)-(O13W)^{i}	1.578(16)
(V3)-(O12)^{i}	1.928(8)	(V4)-(O11)^{v}	1.910(6)	(O13W)-(K1)^{ii}	2.335(14)		
(V3)-(O12)^{i}	1.928(8)	(V4)-(O12)^{v}	1.86(4)	(O13W)-(K1)^{ii}	1.578(16)		

NHVOx

(V1)-(O1)^{i}	1.80(2)	(V2)-(O2)^{i}	1.643(20)	(O8W)-(O1)^{i}	2.08(4)	(N1)-(O1)^{i}	1.959(8)
(V1)-(O2)^{i}	2.037(19)	(V2)-(O3)^{ii}	2.434(19)	(O8W)-(O2)^{i}	2.84(3)	(N1)-(O1)^{i}	1.959(8)
(V1)-(O2)^{ii}	2.476(18)	(V2)-(O3)^{v}	1.941(5)	(O8W)-(O5)^{i}	1.79(3)	(N1)-(O4)^{i}	1.87(3)
(V1)-(O3)^{i}	2.03(3)	(V2)-(O3)^{v}	1.941(5)	(O8W)-(N1)^{i}	2.82(3)	(N1)-(O5)^{v}	2.14(4)
(V1)-(O4)^{i}	1.943(5)	(V2)-(O4)^{v}	2.24(3)	(O8W)-(N1)^{i}	2.82(3)		
(V1)-(O4)^{i}	1.943(5)	(V2)-(O5)^{i}	2.05(2)				

***Symmetry codes**: i = x, y, z; ii = -x, y, -z; iii = -x, -y, -z; iv = x, -y, z; v = x+1/2, y+1/2, z; vi = -x+1/2, y+1/2, -z; vii = -x+1/2, -y+1/2, -z; viii = x+1/2, -y+1/2, z.*

Table S5. Assignment of the Raman vibrational spectra of **NHVOx**, **KVOx** and **NaVOx**.

Symmetry species	NHVOx (cm^{-1})	KVOx (cm^{-1})	NaVOx (cm^{-1})
B_{1g}, B_{3g}	164	164	164
B_{1g}	228	235	-----
B_{1g}, B_{3g}	266	266	266
A_g	399	399	414
B_{2g}	511	506	509
B_{1g}, B_{3g}	676	676	686
B_{2g}	943	957	-----
A_g	1017	1010	1000

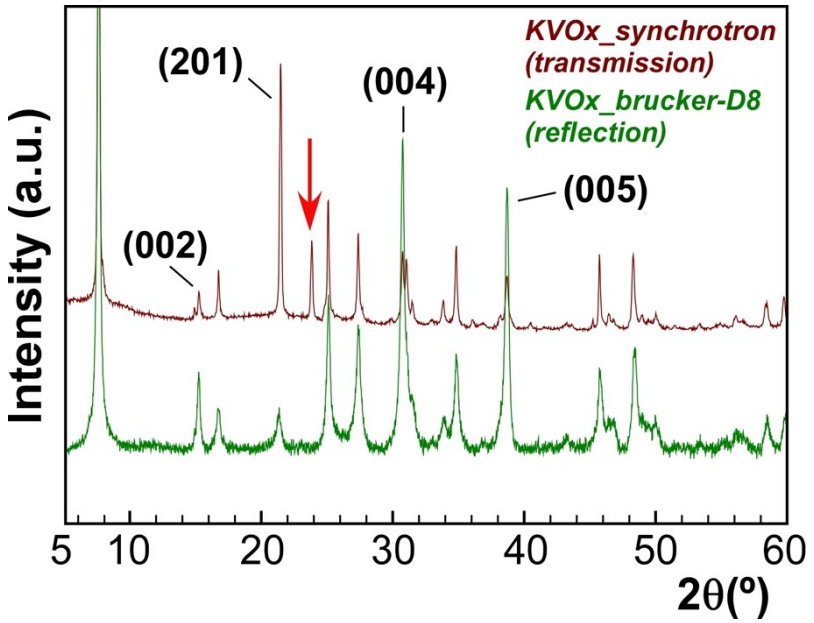

Figure S1. Spurious peak marked with a vertical red arrow observed in the synchrotron X-ray diffraction pattern of **KVOx**. Comparison with the pattern measured in a Brucker D8 Advance diffractometer (CuKα) where the peak does not appear. The wavelength of the synchrotron pattern was changed to CuKα for comparison.

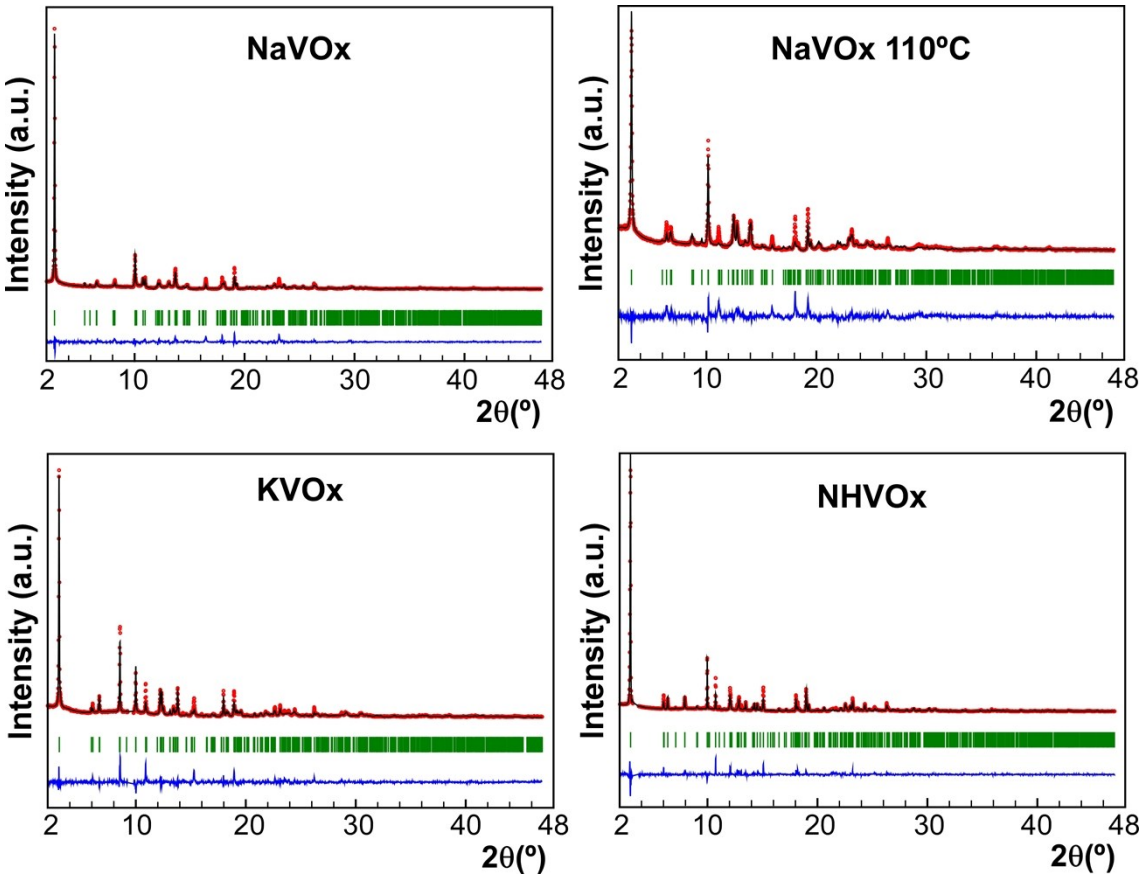

Figure S2. Observed (red dots), calculated (black lines) and difference X-ray powder diffraction patterns (blue lines) for the Rietveld analysis of the phases.

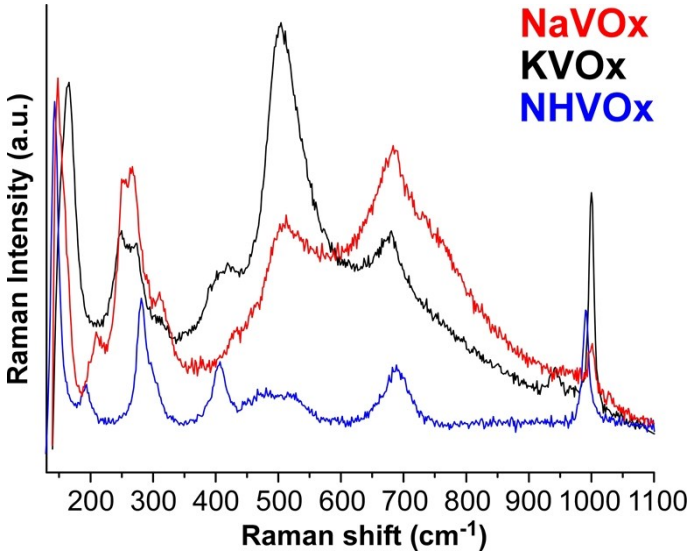

Figure S3. Raman spectra of the phases with the power increased to 50% of the incident laser beam.

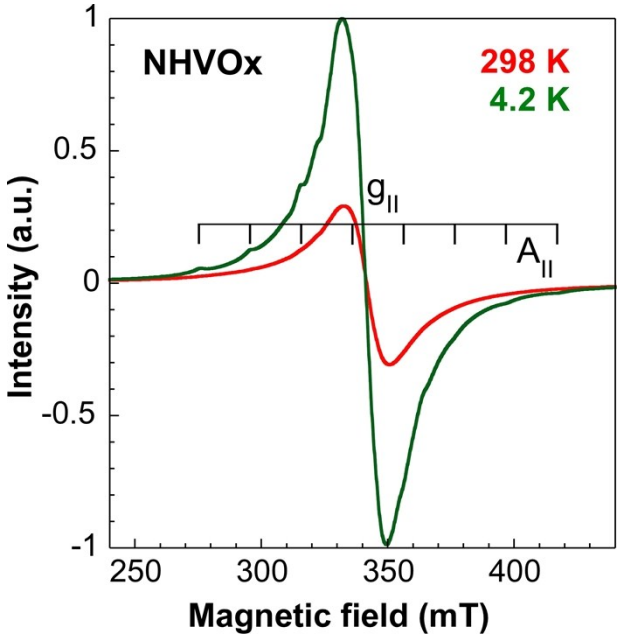

Figure S4. X-band EPR powder spectra at room temperature and 4.2K for **NHVOx.**

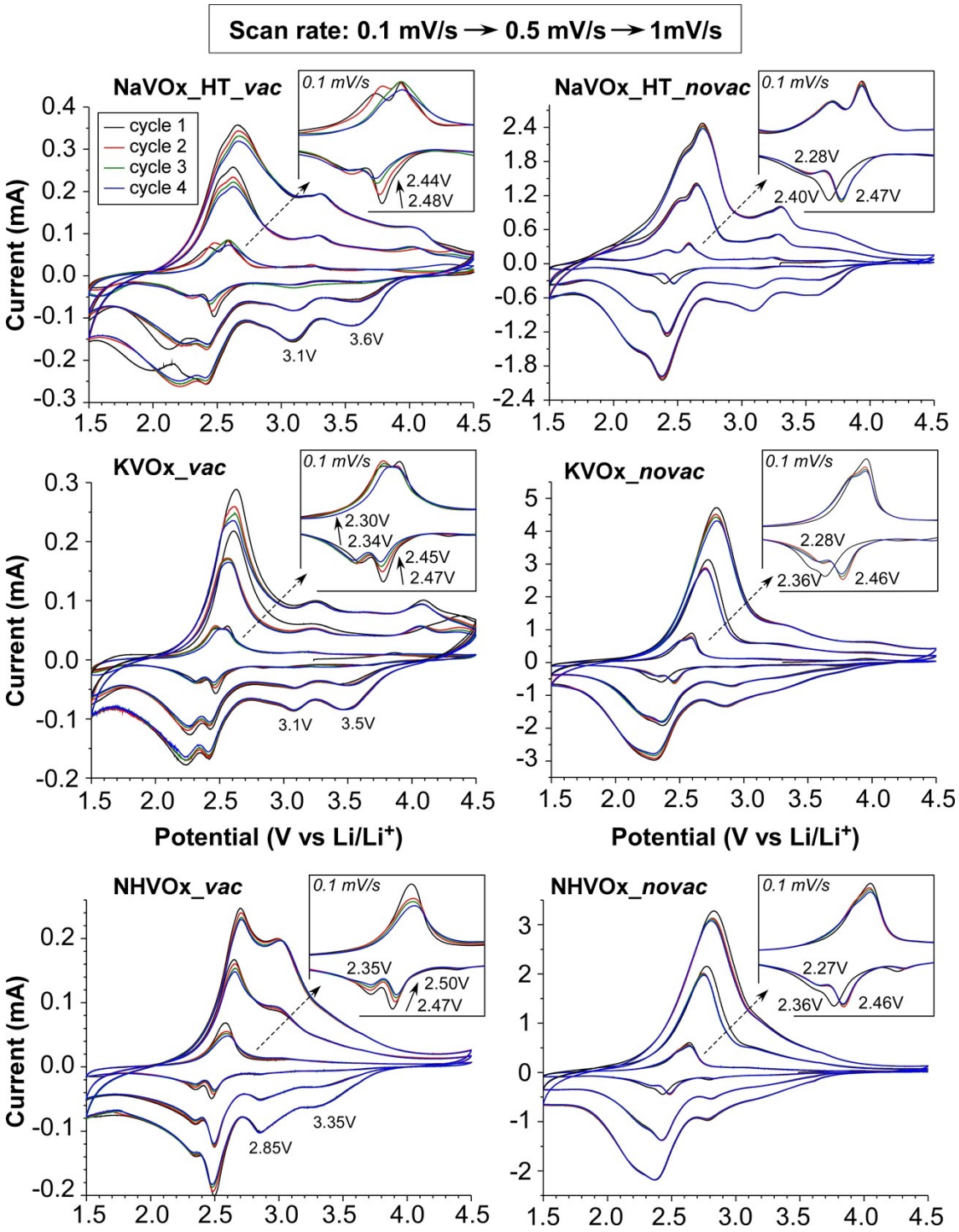

Figure S5. Cyclovoltammetries at different scan rates (0.1 mV/s, 0.5 mV/s and 1mV/s) of the *_vac* and *_novac* electrodes.

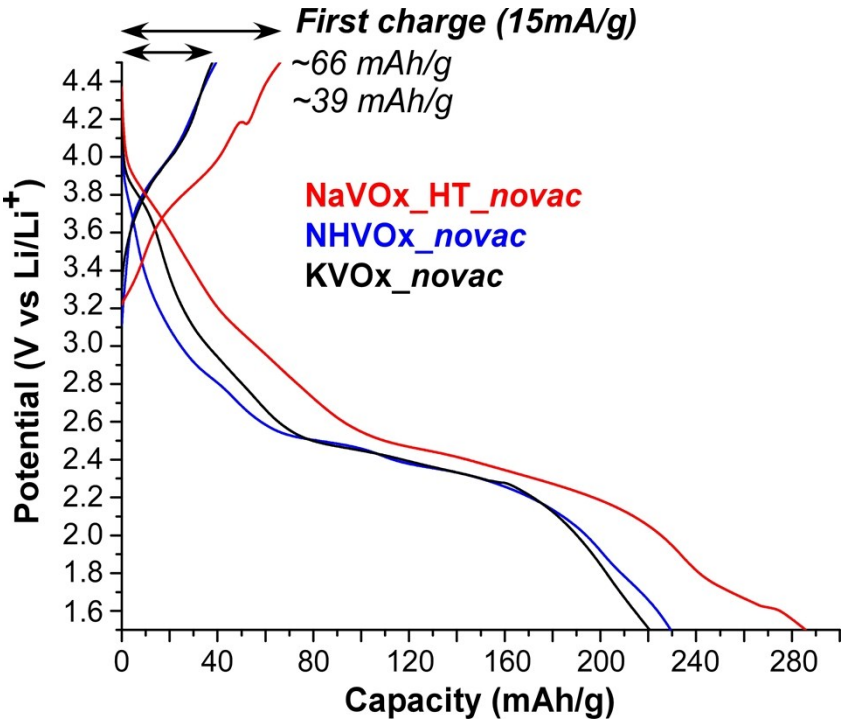

Figure S6. First charge-discharge at 15 mA/g of **NaVOx_HT_*novac***, **NHVOx_*novac*** and **KVOx_*novac*** electrodes.

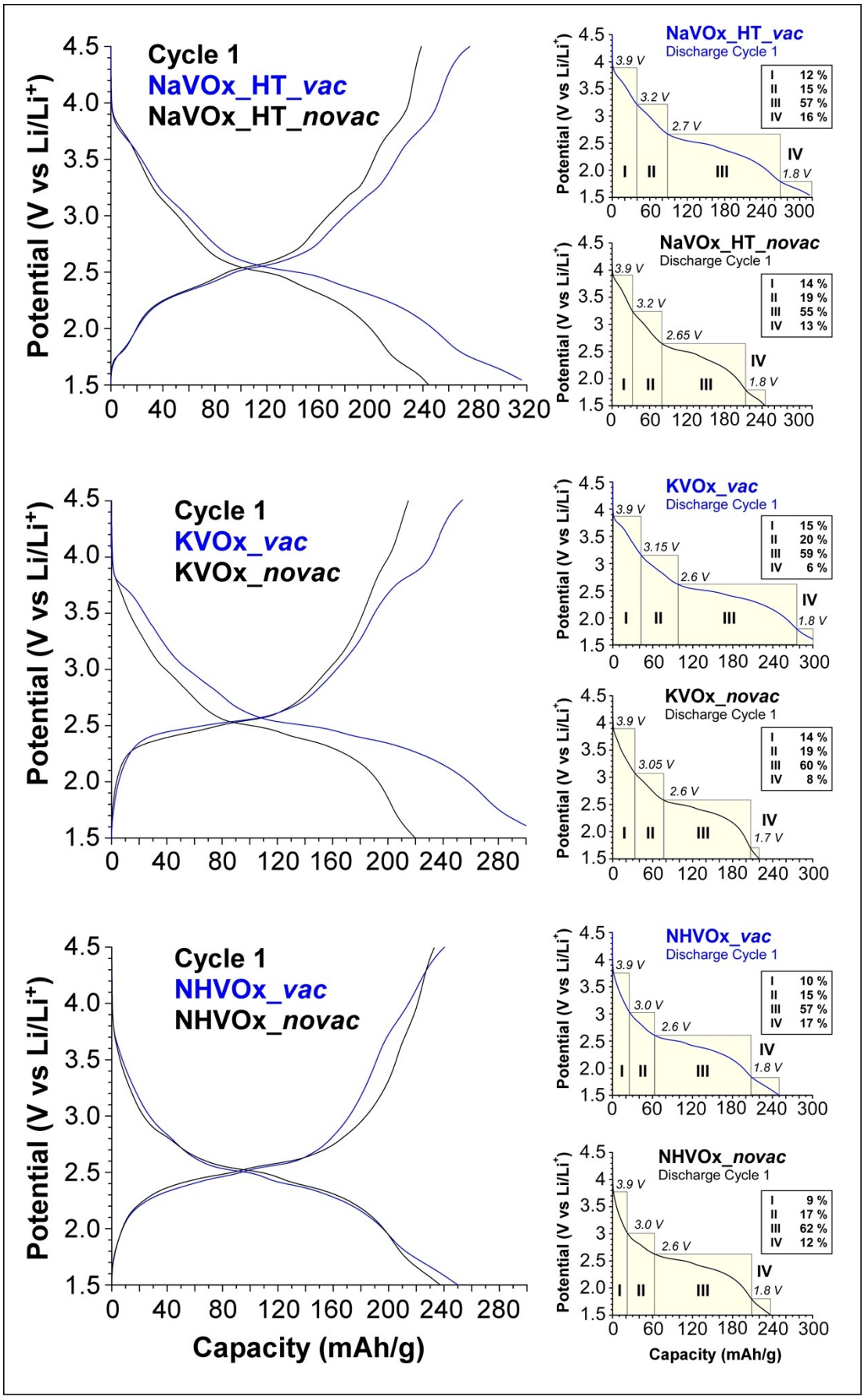

Figure S7. First cycle at 15 mA/g after the cell being discharged to 1.5 V.

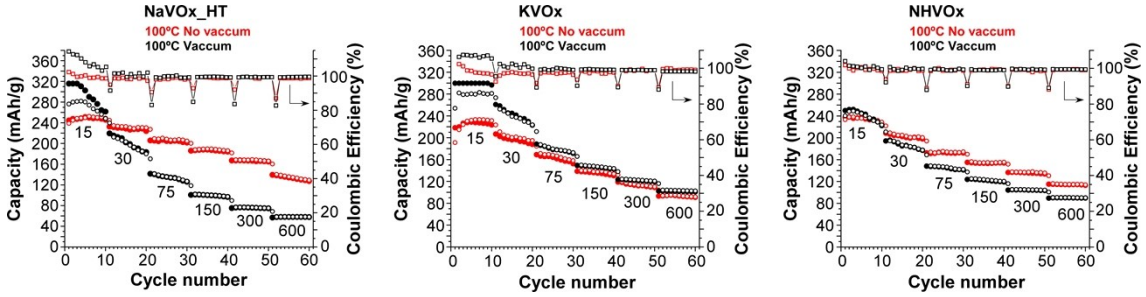

Figure S8. Rate capabilities and the corresponding coulombic efficiencies of the compounds, comparing *_vac* and *_novac* electrodes, recorded at current rates of 15, 30, 75, 150, 300 and 600 mA/g.

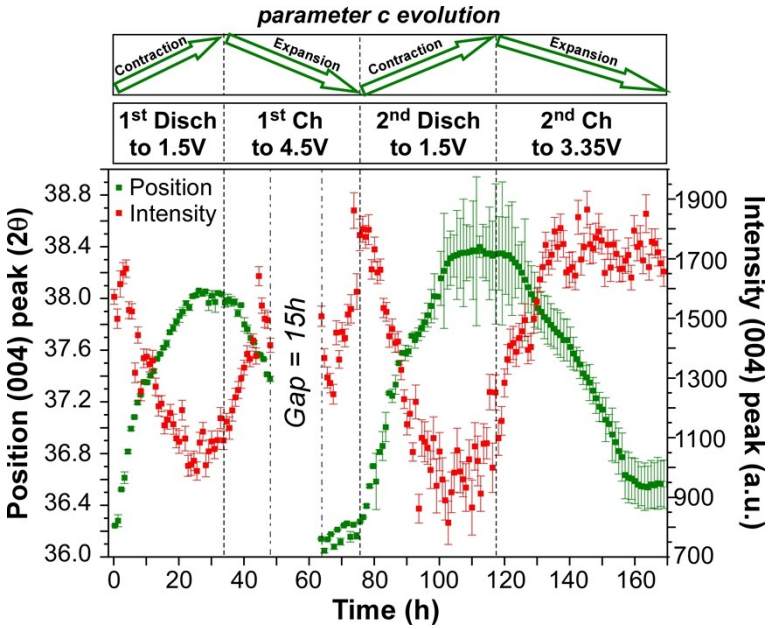

Figure S9. Evolution of the (004) peak position and intensity during the first two discharge-charge cycles of the cell of **KVOx**.

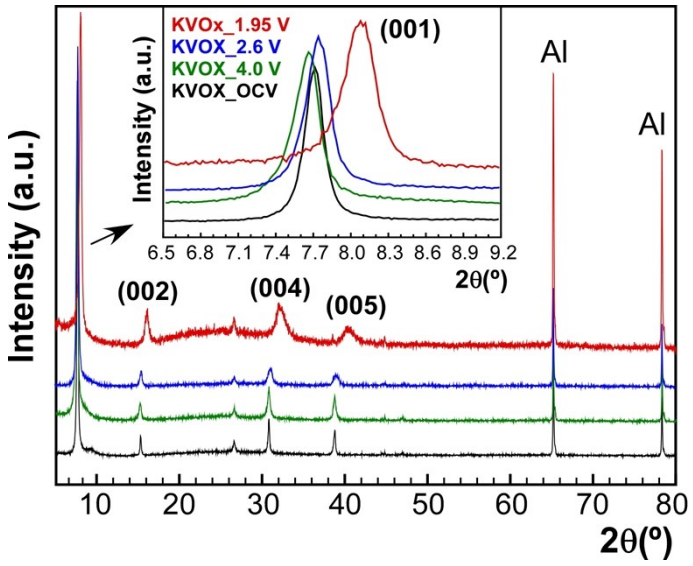

Figure S10. Ex-situ X-ray diffraction patterns of **KVOx** after charging at 15 mA/g to 4.0 V and discharging to 2.6 V and 1.95 V. The patterns were recorded with CuKα.

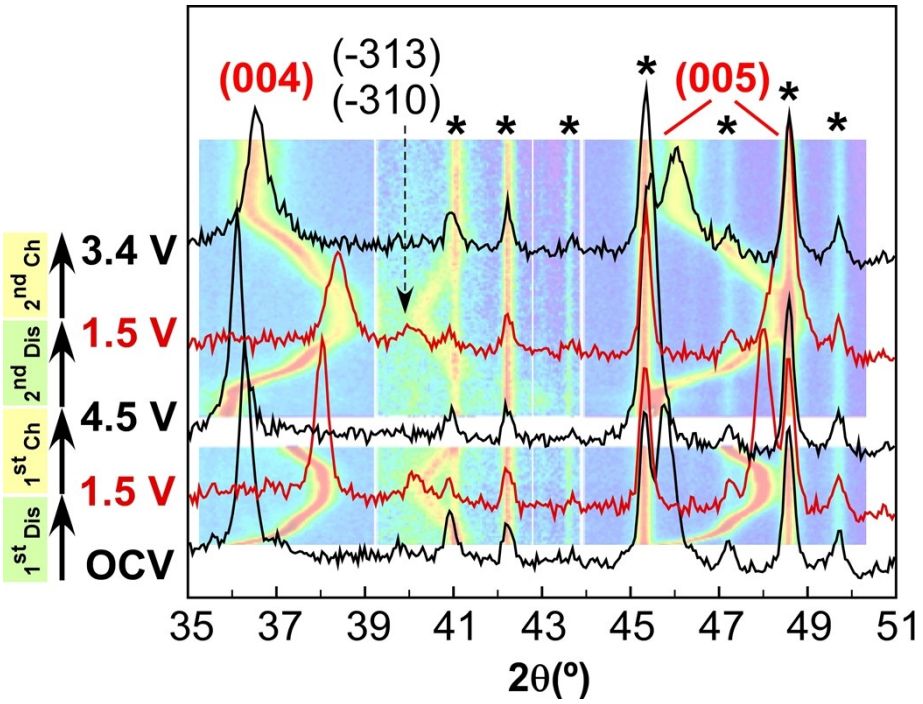

Figure S11. Detailed plot of the XRD patterns between 35 ⩽ 2θ ⩽ 51° during the first two cycles of the cell of **KVOx**. The asterisks represent artifacts of the cell.

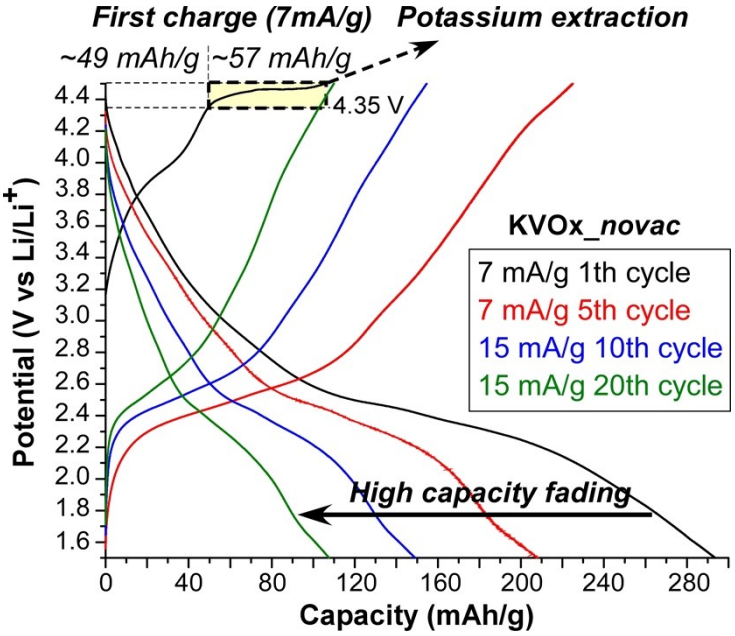

Figure S12. Potassium extraction from the first cycle at very low current density of 6 mA/g for **KVOx_*novac***.

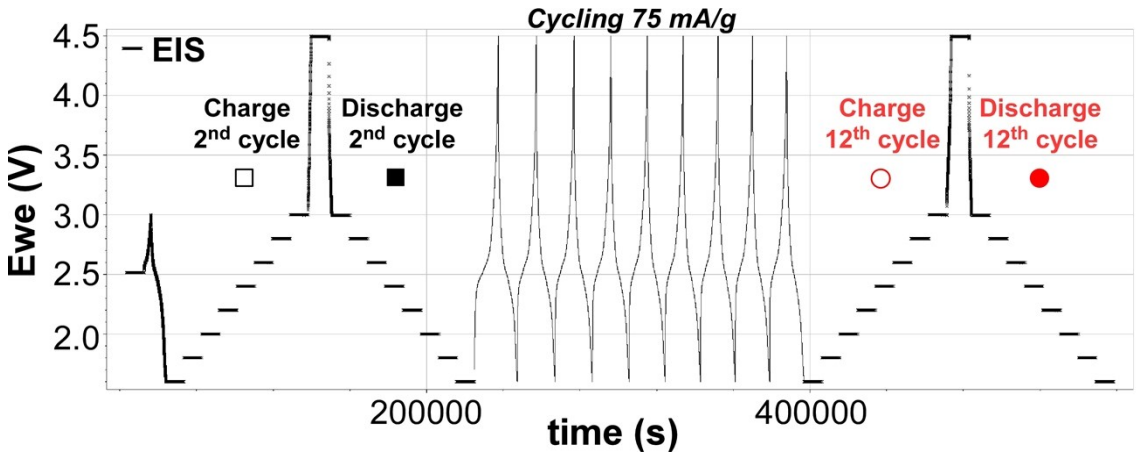

Figure S13. Scheme of the EIS measurement.

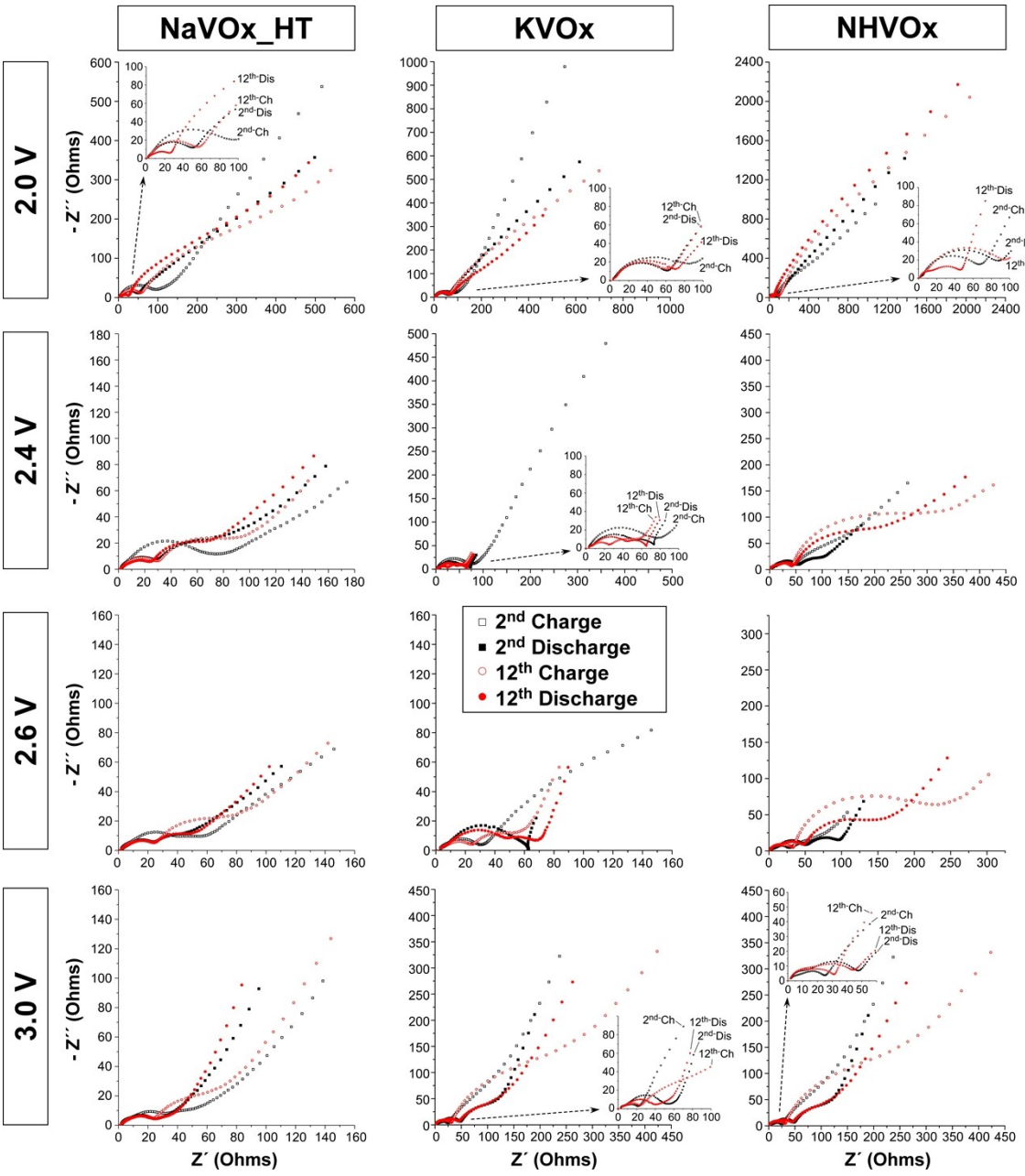

Figure S14. EIS of the phases.

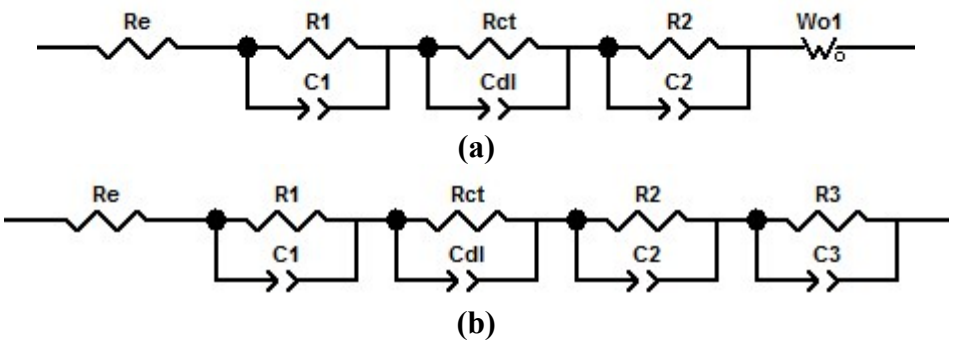

Figure S15. EIS Equivalent circuits for the phases.